

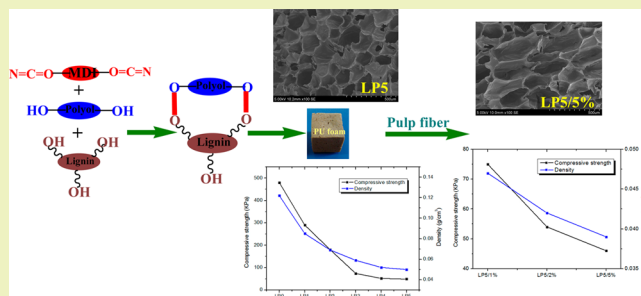
Lignin-Based Rigid Polyurethane Foam Reinforced with Pulp Fiber: Synthesis and Characterization

Bai-Liang Xue,[†] Jia-Long Wen,[†] and Run-Cang Sun^{*,†,‡}[†]Beijing Key Laboratory of Lignocellulosic Chemistry, Beijing Forestry University, Beijing, China[‡]State Key Laboratory of Pulp and Paper Engineering, South China University of Technology, Guangzhou, China

Supporting Information

ABSTRACT: Petroleum-based polyol was replaced with different amounts of lignin (8.33–37.19% w/w) to prepare lignin-based rigid polyurethane foam (LRPF). The LRPF containing 37.19% lignin was further reinforced with different weight ratios (1, 2, and 5 wt %) of pulp fiber. The resulting foams were evaluated by their chemical structure, cellular structure, density, compressive strength, and thermal property. Fourier transform infrared (FT-IR) and ¹³C CP/MAS NMR spectra indicated that typical urethane linkages in LRPF were formed. Scanning electron microscope (SEM) results showed that the cell shape is significantly affected by the lignin and pulp fiber contents, which resulted in inhomogeneous, irregular, and large cell shapes and further decreased the densities of the LRPF. Mechanical results suggested that the compressive strength of the LRPF decreased with the increase in lignin content, but the additional pulp fiber had no significant effect on the compressive strength. Thermogravimetric analysis results demonstrated that the introduction of lignin led to high “carbon residue”, but the introduction of pulp fiber would slightly improve the thermal stability of the LRPF.

KEYWORDS: Lignin, Polyurethane foam, Pulp fiber, Compressive strength, Thermal stability



INTRODUCTION

Lignin, the second most abundant component in the plant cell wall of lignocellulosic materials, is an amorphous polymer that is composed of three different types of phenylpropane units.^{1,2} The pulp and paper industry has generated approximately 55 million tons of lignin each year since 2010, most of which was burned to recover the pulping chemicals and energy.³ To date, the existing markets for lignin products are still quite limited (~2%) with only few lignin-based commodity materials focusing primarily on low value-added products because of its complex structure, low reactivity, and poor processability,⁴ such as agents for dispersing, binding, and emulsion stabilization.⁵ As a natural polymer, lignin contains a large number of aliphatic and phenolic hydroxyl groups, leading researchers to prepare lignin-modified phenolic resin, epoxy polymer, acrylics, and polyurethane (PU).^{6–8}

PU is usually synthesized through a polyaddition reaction between polyfunctional alcohols (polyol polyether or polyol polyester) and polyisocyanate to form urethane linkages. Currently, both the polyisocyanates and polyols are mostly derived from petroleum oil. PU has rapidly grown to be one of the most widely used synthetic polymers with a continuously increasing global market. It has varied applications in different areas, including liquid coatings and paints, adhesives, tough elastomers, rigid foams, flexible foams, and fibers.⁹ Rigid PU foam is a highly cross-linked polymer with a closed-cell structure, which is typically made from methylene diphenyl

diisocyanate (MDI) and polyols. These materials offer low density, thermal conductivity, moisture permeability, and high dimensional stability leading to wide applications in construction, refrigeration appliances, and technical insulations.^{8,10}

Because the aliphatic and phenolic hydroxyl functionalities of lignin can provide good reacting sites toward isocyanates, several attempts have been made to use lignin as polyols for the synthesis of PU.^{5,11,12} Kraft lignin was first incorporated into a polyether triol, forming a cross-linked network of PU.¹³ Rigid PU foam was also prepared from kraft lignin using poly(ethylene glycol) as the solvent.¹⁴ PU containing low lignin content exhibited considerable toughness at specific values of [NCO]/[OH] ratios, while the corresponding PU with high lignin contents (>30 wt %) were hard and brittle, regardless of the [NCO]/[OH] ratio used.¹³ Generally, PU prepared with a low molecular weight lignin was more flexible than those made of medium or high molecular weight lignin. However, when the kraft lignin content in PU was higher than 30 wt %, rigid and glassy products were obtained, regardless of the low molecular weight of the lignin being used.¹⁵ Moreover, lignin possesses a unique thermal stability. For example, the acetic acid lignin-containing PU showed that its thermal stability was improved with increasing lignin content; however, a maximum lignin

Received: February 21, 2014

Revised: May 1, 2014

Published: May 12, 2014

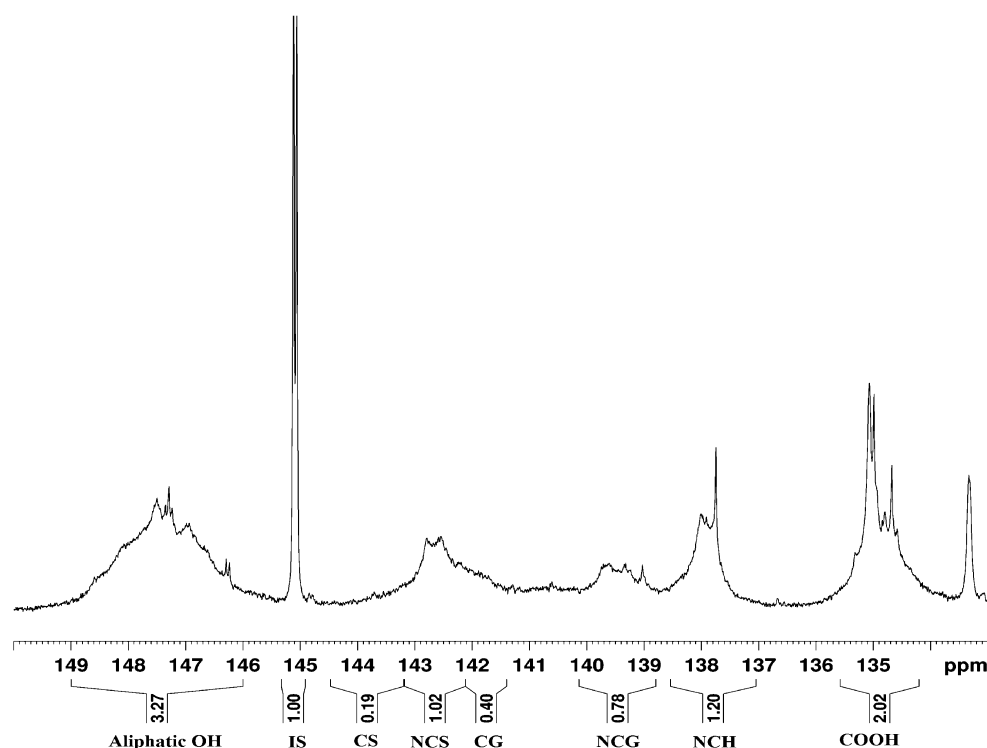


Figure 1. ^{31}P NMR spectra of the lignin. IS, internal standard; CS, condensed syringyl OH; NCS, noncondensed syringyl OH; CG, condensed guaiacyl OH; NCG noncondensed guaiacyl OH; and NCH, noncondensed *p*-hydroxyphenyl OH.

Table 1. Functional Groups and Molecular Weight of Lignin^a

	Ph-OH 148–146 (mmol/g)	Al-OH 143–137 (mmol/g)	total-OH	M_w (g/mol)	M_n (g/mol)	M_w/M_n
lignin	3.59	3.27	6.86	2790	909	3.07
PEG-400	5.75		5.75			

^aNote: Ph-OH, phenolic hydroxyl group; Al-OH, aliphatic hydroxyl group; M_w , weight average molecular weight; and M_n , number average molecular weight.

content of 43.3% can be reached for the continuous film formation.¹⁶

It is well known that lignocellulosic fibers contain lots of hydroxyl groups, and this unique nature draws considerable interest to reactive composite formulations of typically rigid PU foam. It also decreased the environmental impact after disposal due to its susceptibility to fungal attack in wet environments.¹⁷ The incorporation of lignocellulosic fibers into the petroleum-based rigid PU foam was recently reported.^{18,19} Banik et al. have investigated the effect of refined cellulose fiber from bleached kraft pulp on the mechanical property of rigid PU foam.¹⁸ The effect of maple pulp fiber on the mechanical and thermal property of the soy-based rigid PU foam had been also evaluated.¹⁹ However, to our best knowledge, few researches have directly discussed the addition of pulp fiber content on the mechanical property and thermal stability of the LRPF to obtain eco-friendly materials.

In the present work, lignin was evaluated to replace the polyol for the preparation of LRPF. The effect of lignin content on the biofoam preparation and properties (density, compressive strength, and cellular structure) was investigated. Furthermore, optimal LRPF reinforced with different amounts of pulp fiber was first prepared and then evaluated. Fourier transform infrared spectra (FT-IR), scanning electron microscope (SEM) micrograph, and density, as well as the mechanical and thermal properties of the biofoams were investigated.

■ MATERIALS AND METHODS

Materials. Methyl-diphenyl diisocyanate (MDI-50) with 50% 4, 4-isomers and 50% 2,4-isomers was supplied by Yantai Wanhua Co., Shandong, China. NCO is the concentration of isocyanate groups in the MDI (7.50 mmol/g). Poly(ethylene glycol) of molecular weight 400 g/mol (PEG-400) was used as the polyether polyol. The content of hydroxyl groups in PEG-400 (5.75 mmol/g) was quantified by ^{31}P NMR. Di-*n*-butyltin dilaurate (DBTDL), a catalyst used in manufacturing PU foam, was obtained from Sinopharm Chemical Reagent Co., Shanghai, China. AK-8801, a silicone surfactant used to stabilize the foam, was a commercial product from Dymatic Shichuang Chemical Co., Nanjing, China. Distilled water was used as a blowing agent. Lignin, extracting with mild alkaline solution from the corn cob residue after hydrolysis of hemicelluloses, was supplied by the Longlive Biological Technology Co., Shandong, China. The alkaline lignin contained 94.65% Klason lignin, 5.02% acid-soluble lignin, and 0.33% polysaccharides (cellulose). Pulp fibers were obtained from Donghua Pulp Factory, Beijing, China. The pulp fiber particle size was in the range of 500–850 μm (60–80 mesh). All these commercial products were used as received without any further treatment.

Characterization of Lignin. The chemical composition analysis of alkaline lignin was determined by the Klason protocol according to TAPPI standard method T-222. In brief, the lignin samples were treated with 72% sulfuric acid for 1 h at 30 °C, diluted to 3% sulfuric acid using deionized water, and subsequently autoclaved at 121 °C for ~1 h. The resulting solution was cooled to room temperature, and the precipitate was then filtered, dried, and weighed to get the Klason lignin content. The resulting filtrate was used for the detection of sugar composition by high-performance anion exchange chromatography

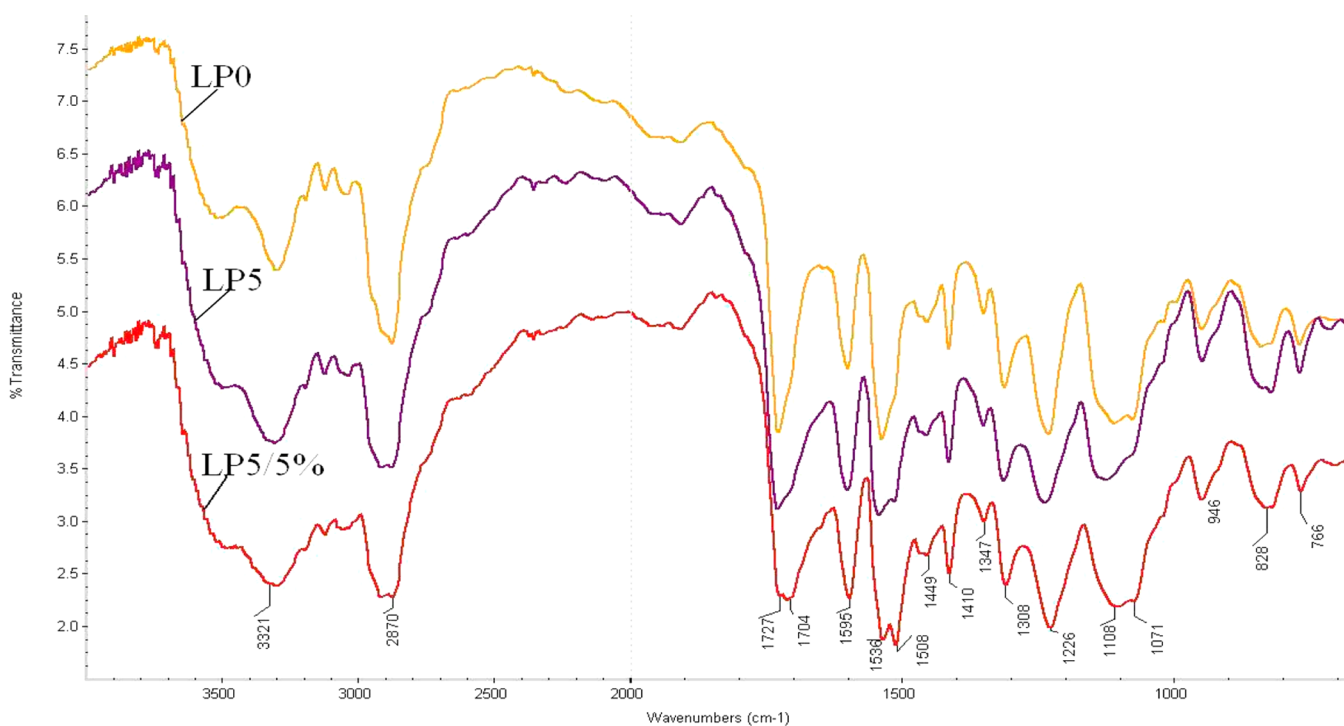


Figure 2. FT-IR spectra of the biofoams.

(HPAEC-PAD) using Dionex ICS-3000 (Dionex Corp., U.S.A.), and the acid-soluble lignin was measured by ultraviolet spectroscopy.

Quantitative ^{31}P NMR spectrum of the lignin was obtained using the published procedures.²⁰ ^{31}P NMR spectra were recorded with 65,536 data points and a spectral width of 32,467 Hz. A relaxation delay of 5 s was used, and the number of scans was 1024. The pulse program named “zg30” was used. Samples (20 mg) were dissolved in 500 μL of anhydrous pyridine and deuterated chloroform (1.6:1, v/v) under constant stirring. This was followed by the addition of 100 μL of cyclohexanol (10.85 mg/mL) as an internal standard and 50 μL of chromium(III) acetylacetonate solution (5.0 mg/mL in anhydrous pyridine and deuterated chloroform 1.6:1, v/v) as a relaxation reagent. Finally, these mixtures were treated with 100 μL of phosphitylation agent (TMDP) (2-chloro-4,4,5,5-tetramethyl-1,3,2-dioxaphospholane) and was transferred into a 5 mm NMR tube for subsequent NMR analysis. All NMR experiments were carried out on a Bruker AV III NMR spectrometer at 400 MHz at 25 $^{\circ}\text{C}$. Spectra were processed and analyzed using the Bruker Topspin 2.1 software package.

Gel permeation chromatography (GPC, Agilent 1200, U.S.A.) was carried out on a PL-gel mixed bed HPLC column (inner diameter, 7.5 mm; length, 300 mm; particle size, 10 μm ; midweight range, 500–10 M). Detection was achieved with a Knauer differential refractometer. The column was eluted with tetrahydrofuran at a flow rate of 1.0 mL/min. Samples (4 mg) were dissolved in 2 mL tetrahydrofuran.

Procedure for Biofoam Preparation. LRPF was prepared by a one-shot method according to the formulation listed in Table S1 of the Supporting Information. The $[\text{NCO}]/[\text{OH}]$ ratio of the systems was set at 1.05. The polyol was first mixed with the additives (lignin, catalyst, surfactant, and blowing agent) at an ambient temperature for 5 min, and then all the ingredients were thoroughly mixed manually using a glass rod to disperse different amounts of the lignin in the polyol. Afterward, predetermined MDI was added into the paper cup and stirred vigorously with a high speed mixer (2000 rpm) for 30 s. Finally, the resultant mixture was quickly poured into a cubic paper container at room temperature to produce the biofoams. The biofoam without lignin was prepared as a control following the same procedure aforementioned, named LP0. For the preparation of LRPF, the amounts of lignin and polyol were determined by different molar ratios of the hydroxyl groups from lignin to those from polyol (1:9, 2:8, 3:7, 4:6, and 5:5), which corresponded to the samples LP1, LP2, LP3, LP4,

and LP5. For the preparation of LRPF reinforced with pulp fiber, the pulp fiber was manually premixed with polyol for 10 min to ensure complete penetration. Sample LP5 was selected as the substrate, which was reinforced by varying the amount of pulp fiber. The biofoams obtained containing 1, 2, and 5 wt % pulp fiber (based on the weights of lignin and polyol) were successfully prepared and coded as LP5/1%, LP5/2%, and LP5/5%, respectively.

The amounts of lignin, polyol, and MDI were determined according to the molar ratios of isocyanate to hydroxyl (NCO/OH) calculated using the equation below

$$\text{NCO/OH} = W_{\text{MDI}}[\text{NCO}]_{\text{MDI}} / (W_{\text{L}}[\text{OH}]_{\text{L}} + W_{\text{P}}[\text{OH}]_{\text{P}})$$

W_{MDI} , W_{L} , and W_{P} represent the weights (g) of MDI, lignin, and polyol, respectively. $[\text{NCO}]_{\text{MDI}}$ is the molar content of the isocyanate groups in MDI. $[\text{OH}]_{\text{L}}$ and $[\text{OH}]_{\text{P}}$ are the molar contents of total hydroxyl groups in the lignin and polyol, respectively.

Measurements. *Density Measurement.* Apparent density of the PU foam was measured according to ASTM D1622-03. The size of the specimen was 30 mm \times 30 mm \times 30 mm (length \times width \times thickness). The average values of five specimens per sample were reported.

Fourier Transform Infrared Spectroscopy. FT-IR spectra were recorded using a Thermo Scientific Nicolet iN10 FT-IR microscope (Thermo Nicolet Corporation, Madison, WI) equipped with a liquid nitrogen-cooled MCT detector. Samples were ground and pelletized using BaF_2 , and their spectra were recorded in the range from 4000 to 700 cm^{-1} at 4 cm^{-1} resolution and 128 scans per sample.

Solid-State ^{13}C CP/MAS NMR Spectroscopy. Solid-state ^{13}C CP/MAS NMR analyses of the PU foams were carried out at 100 MHz on a Bruker Avances 400 spectrometer with MAS at 5 kHz. The pulse width was 1 μs , and delay time is 2s. The number of scans is 5000. Approximately 40 mg of sample was packed in a zirconium sample tube.

Scanning Electron Microscope. Samples were coated by a sputter-coating (BOT 341F) with evaporated gold, and subsequently, the morphology was examined using a SEM (Hitachi S-3000, Hitachi High Technologies, Inc., Tokyo, Japan) at an acceleration voltage of 15 kV.

Mechanical Tests. Compressive strengths of the foams were measured at ambient conditions with a universal testing machine (Zwick Universal testing machine Z005). The size of the specimen was

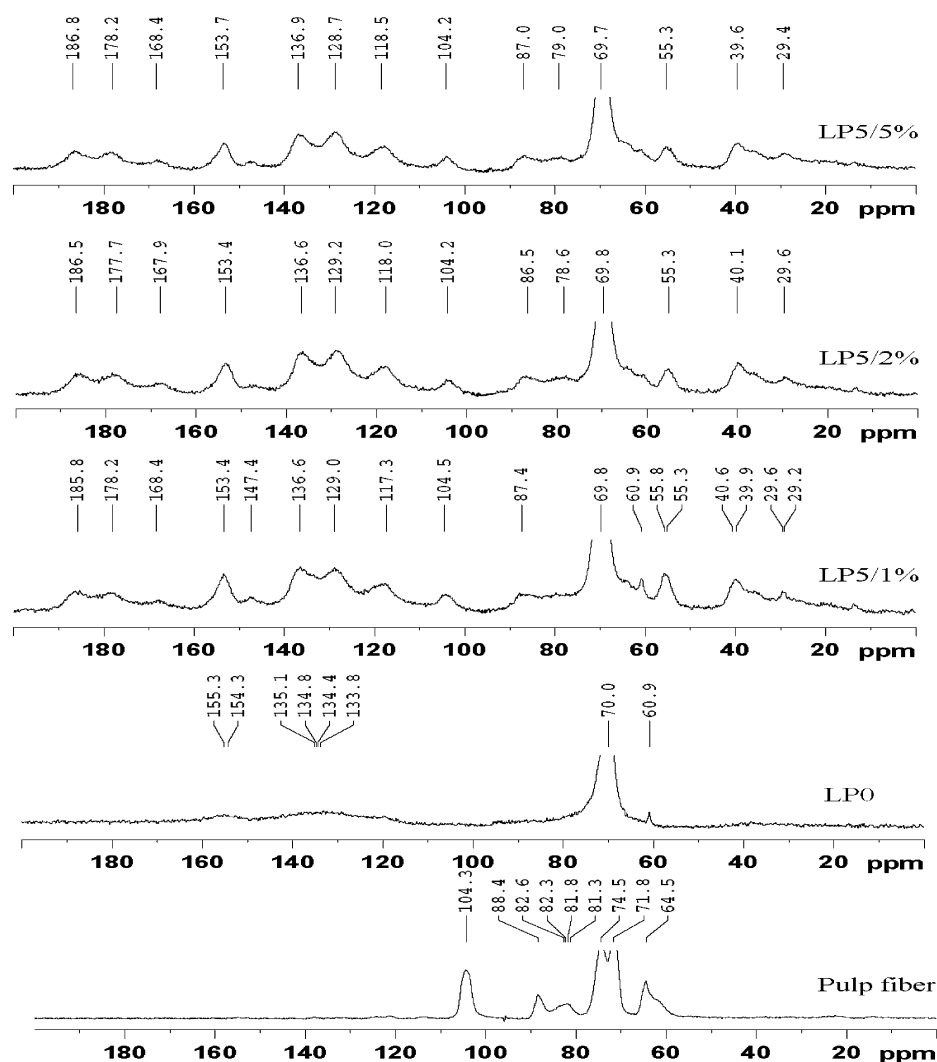


Figure 3. ^{13}C CP/MAS NMR spectra of biofoams.

30 mm \times 30 mm \times 30 mm (length \times width \times thickness), and the rate of crosshead movement was fixed at 2 mm/min for each sample. Compressive stress at 10% strain in parallel to foam rise direction was performed according to ASTM D1621-10. For each compressive test, five replicate specimens were tested, and an average value was taken along with the standard deviation.

Thermogravimetric Analysis. Thermogravimetric analysis (TGA) experiments were performed using a simultaneous thermal analyzer (SDT Q600 TGA/DSC, TA Instrument). Ten milligrams of each sample was heated from room temperature to 600 $^{\circ}\text{C}$ at a heating rate of 10 $^{\circ}\text{C}/\text{min}$ under an inert atmosphere of nitrogen.

RESULTS AND DISCUSSION

Preparation of Biofoams. The hydroxyl value and molecular weight of the lignin are the two important parameters in preparing the LRPF. The ^{31}P NMR spectra of lignin are shown in Figure 1, and their phenolic and aliphatic hydroxyl values and molecular weight data are summarized in Table 1. It is suggested that the lignin had a suitable hydroxyl value used as a polyol. Moreover, its molecular weight was relatively low, which was comparable with the lignin obtained from other lignocelluloses.²¹ Thus, this kind of lignin could be used as a potential alternative resource for the preparation of the LRPF. The content of lignin added in the PU foam matrix is calculated based on the molar ratio of the hydroxyl groups from lignin to

those from polyol (Table S2, Supporting Information). The maximum content of lignin added into the biofoam was 37.19% (w/w). To evaluate the effects of pulp fiber on the cell morphologies and mechanical and thermal properties, the LRPF with the maximum lignin addition was further reinforced by different amounts of pulp fiber (1–5%). The addition of pulp fiber could influence the lignin in dispersing the polyol and further affect the generation of the bubbles of CO_2 . Thus, the maximum addition of pulp fiber content into the LRPF was selected as 5%. Representative photographs of samples LP0 and LP5 are shown in Figure S1 of the Supporting Information. It is clear that the biofoam shows a brown color after introduction of the lignin in the biofoam.

Chemical Structure of Biofoams. FT-IR spectroscopy was used to study the chemical structures of PU foams. As shown in Figure 2, the urethane moieties of PU foam were confirmed by the presence of the main characteristic absorption bands: $\text{OC}=\text{O}$ vibration absorption at 1727 cm^{-1} , $\text{CO}-\text{NH}$ vibration absorption at 1595 cm^{-1} and $\text{N}-\text{H}$ bending vibration absorption at 1536 cm^{-1} .²² These features indicated the occurrence of chemical interaction between the hydroxyl groups of lignin and MDI in the samples (LP0 and LP5). The carbonyl absorption band was split into two peaks, 1727 and 1704 cm^{-1} , corresponding to free and hydrogen-bonded carbonyl groups,

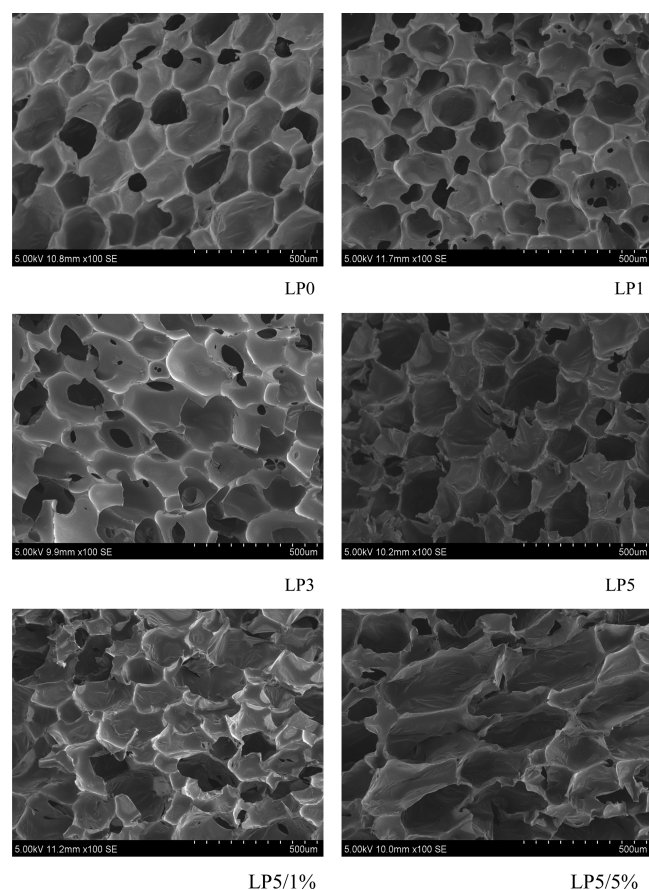


Figure 4. SEM images of the cross-section of different PU foams.

respectively. The free carbonyl group was obviously present in the samples (LP0 and LP5); however, the stretching vibration absorption of the carbonyl group shifted mildly from 1727 to 1704 cm^{-1} in sample LP5/5% after the addition of pulp fiber, suggesting that the formation of hydrogen bonds was partially existing between polar groups in the pulp fiber and MDI.²³ Moreover, the apparent peak at 1508 cm^{-1} in sample LP5/5% is probably attributed to N–H bending deformation combined with C–N asymmetric stretching, providing additional evidence for the chemical reaction of the hydroxyl groups of pulp fiber with MDI through covalent bonds.²⁴ Additionally, the bands at 1595 and 1536 cm^{-1} correspond to the aromatic skeletal vibrations of lignin; their relative intensities were rather similar in the spectra of samples LP5 and LP5/5%, indicating that the typical structures of lignin did not alter appreciably during the reaction.²⁵

¹³C CP/MAS NMR spectra of the biofoams are shown in Figure 3. The spectrum of the pulp fiber consists of the following resonances: 104.3 (C-1), 88.4 (C-4), 74.5 (C-5), 81.8 (C-3), 71.8 (C-2), and 64.5 ppm (C-6), indicating that it is a typical cellulose I.²⁶ The feature of the lignin structure in the biofoams was also identified, although the signal intensities in the aromatic region (110 – 160 ppm) were weak. The spectra showed the typical lignin featured with a relatively high proportion of β -aryl ether linked by syringyl units (C-3/5 in syringyl units, 153 ppm). The peak at 136 ppm represented C-1 in syringyl units.²⁹ The typical lignin features revealed by the ¹³C CP/MAS NMR spectra suggested that the basic structures of lignin did not change during the preparation of the biofoams. In the spectra of the LRPF containing different amounts of pulp

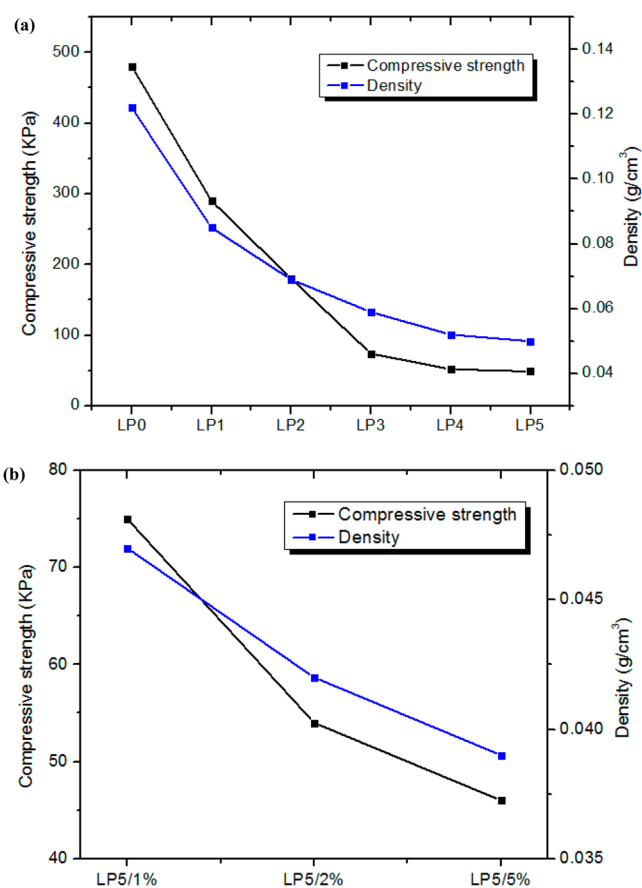


Figure 5. Density and compressive property of different PU foams.

fiber, the signals at 88.4 and 64.5 ppm, attributing to the C-4 and C-6 of crystalline cellulose, basically disappeared as compared to those of the pulp fiber, suggesting that the chemical reaction between the pulp fiber and MDI indeed occurred after the addition of pulp fiber into the biofoams.²⁷

Morphological Structures of Biofoams. SEM images of the cross-section of different PU foams are shown in Figure 4. The pore surface of neat PU was mostly regular and smooth. The cellular structure of the LRPF was closely related to the content of lignin in the PU matrix; with the increase in lignin content, the cellular shape became more inhomogeneous and less regular along with extra formation of large cells. The alteration in the cell morphology was probably due to the fact that the lignin may affect the process of cell nucleation in preparation of PU foams.²⁸ Additionally, it was noted that the cell structure of the sample LP5 was obviously different from that of the sample LP1 and LP3. This was probably because the lignin did not disperse well in the PU foam once the content of lignin reached 37.19% . In the SEM images of samples LP5/1% and LP5/5%, the overall cell shape became more irregular, and the cell became larger with increasing addition of pulp fiber content.

Mechanical Property of Biofoams. Apparent density is one of the most important parameters affecting the mechanical properties of biofoams. In contrast with the density of neat PU foam (0.122 g/cm^3) in Figure 5a, the density of samples LP1 and LP2 dropped sharply to 0.085 and 0.069 g/cm^3 , respectively. However, with a further increase in lignin content in the PU foam matrix, the densities did not decline remarkably. The reduced density is mostly related to their morphological

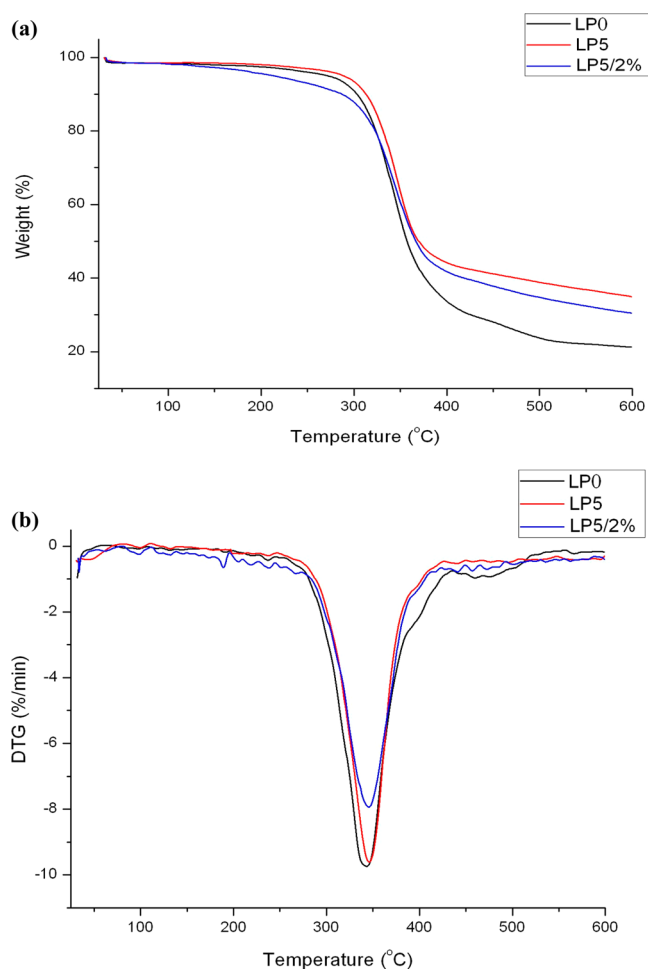


Figure 6. Degradation TGA curves (a) and the rate of weight loss (b) of different PU foams.

characteristics of the LRPF. The increasing addition of the lignin led to the formation of the biofoam with less uniform and larger cells.²¹ Furthermore, when different contents of the pulp fiber were added into sample LP5, the densities also decreased with an increase in the pulp fiber content as shown in Figure 5b. For instance, the addition of 1% pulp fiber into sample LP5 caused the density to reduce to 0.047 g/cm³. The density decreased to 0.042 and 0.039 g/m³ in the LP5/2% and LP5/5%, respectively. These facts suggested that the pulp fibers could influence the reactivity of the components in the system, which affects the foam expansion as well as density. LRPF reinforced with increasing pulp fiber content was accompanied by a slight increase in open-cell content, which corresponded to the SEM results (Figure 4).

Compared to neat PU foam, the compressive strength of the LRPF was significantly reduced with the increase in lignin content. The compressive strength of the LRPF decreased from 290 to 180 MPa with lignin content increased from 8.33 to 16.18%. The reduced compressive strength was due to the relative low amount of hydroxyl groups in lignin, which led to the low cross-linking density and compressive strength of the LRPF as compared to pure polyol. In addition, the lignin was not completely miscible with the polyol, and thus, the introduction of an uneven mixture of lignin and polyol also resulted in an irregular cellular structure, as indicated by SEM pictures. Moreover, the uneven mixture of lignin and polyol

also induce an internal defect of the PU; thus the stress concentration probably occurred, which undoubtedly weakened the compressive strength of the LRPF. Further increasing the addition of the lignin content from 23.61% to 30.62% did not result in apparent decline of compressive strength. These results can be explained by the fact that the lignin macromolecules were prone to self-associate, agglomerate, and form the interpenetrating polymer network instead of chemically interacting with PU chains when excess amounts of lignin were added into the PU foam matrix.²⁹

Compared with sample LP5, the compressive strength of the sample LP5/1% was slightly improved by the addition of 1% pulp fiber due to its stiffness. However, the further increase in pulp fiber content resulted in a slight loss of compressive strength. The lack of reinforcing effect is possibly due to the limited cross-linked action between the pulp fiber and PU, which further affected the biofoam expansion as well as its density, leading to the large cells formed.¹⁷ These results were in agreement with their morphological characteristics in Figure 4. In short, the pulp fiber had no obvious effect on the compressive strength of the biofoams.

Thermal Stability of Biofoams. Thermogravimetric analyses were performed to investigate the effect of the lignin and pulp fiber on the thermal behaviors of the biofoams. As shown from the degradation TGA curves in Figure 6a, all of the samples had a narrow degradable temperature range around 300–400 °C. The initial stage of weight loss was dominated by the degradation of the polyol component and pulp fiber at around 300 °C, and sample LP5/2% had a slight higher initial decomposition rate as compared to LP0 and LP5, suggesting that the presence of the pulp fiber would elevate the initial decomposition temperature.³⁰ The second stage at around 400 °C was mainly attributed to the degradation of urethane structures of the biofoams.¹⁹ It was observed that sample LP0 had a slightly higher decomposition rate than those of samples LP5 and LP5/2%, implying that less urethane linkages formed in samples LP5 and LP5/2% because the amount of accessible hydroxyl groups and active group in lignin is less than in commercialized polyol. Furthermore, sample LP5/2% had a lower decomposition rate than that of LP5. This is probably due to the limited chemical interactions of introduced pulp fiber with PU chains during the polymer reaction. With respect to the “char residues” in the TG curves, it was found that the “char residues” at 600 °C were 36% for LP5, 32% for LP5/2%, and 25% for LP0 in the present study. This fact suggested that the content of “char residues” is related to the lignin content in PU because lignin has higher thermal stability than neat PU (LP0). However, the “char residues” value was slightly decreased in sample LP5/2% because of low thermostable fiber.

The rate of weight loss was reflected in Figure 6b; the maximum weight loss rate of the three samples was around 350 °C. It is interesting to note that the maximum decomposition rates of samples LP0 and LP5 were almost the same; however, the maximum decomposition temperature was improved after the introduction of the pulp fiber into the LRPF (LP5/2%), suggesting that the thermal stability of the biofoam was improved by the addition of the pulp fiber.

Conclusion. In this study, to replace commercial polyol with lignin in traditional PU production, lignin-based rigid PU biofoam with higher lignin content was prepared. The lignin-based biofoam was further reinforced with pulp fiber, and novel biofoam was successfully synthesized. The pulp fiber-reinforced biofoams had larger regular cells as well as lower foam density

due to the pulp fibers embedding in the biofoam. Larger cells and lower density of PU foam are beneficial to the thermal conductivity of PU foam, which has a higher heat transfer ability than that of PU foam with smaller cells. The introduction of the pulp fiber into the lignin-based biofoam did not influence its compressive strength, but its thermal stabilities were slightly improved. The combined application of the lignin and pulp fiber in the synthesis of the biofoam explores a green and economical way to utilize the most abundant natural biopolymers.

■ ASSOCIATED CONTENT

🔍 Supporting Information

Table S1: Formulation of the lignin-based PU foams. Table S2: Lignin content in the lignin-based rigid polyurethane foams. Figure S1: Representative photograph of the samples LP0 and LP5. This material is available free of charge via the Internet at <http://pubs.acs.org>.

■ AUTHOR INFORMATION

Corresponding Author

*Tel: +86-10-62336903. Fax: +86-10-62336903. E-mail: rcsun3@bjfu.edu.cn.

Notes

The authors declare no competing financial interest.

■ ACKNOWLEDGMENTS

We are grateful for the financial support of this research from the Fundamental Research Funds for the Central Universities (BLYJ201312), National Natural Science Foundation of China (31110103902), and Major State Basic Research Projects of China (973-2010CB732204).

■ REFERENCES

- (1) Borges da Silva, E. A.; Zabkova, M.; Araujo, J. D.; Cateto, C. A.; Barreiro, M. R.; Belgacem, M. N.; Rodrigues, A. E. An integrated process to produce vanillin and lignin-based polyurethanes from kraft lignin. *Chem. Eng. Res. Des.* **2009**, *87*, 1276–1292.
- (2) Chakar, F. S.; Ragauskas, A. J. Review of current and future softwood kraft lignin process chemistry. *Ind. Crop. Prod.* **2004**, *20*, 131–141.
- (3) Calvo-Flores, F. G.; Dobado, J. A. Lignin as renewable raw material. *ChemSusChem*. **2010**, *3*, 1227–1235.
- (4) Lora, J. H.; Glasser, W. G. Recent industrial applications of lignin: A sustainable alternative to nonrenewable materials. *J. Polym. Environ.* **2002**, *10*, 39–48.
- (5) Thring, R. W.; Vanderlaan, M. N.; Griffin, S. L. Polyurethanes from Alcell® lignin. *Biomass Bioenergy* **1997**, *13*, 125–132.
- (6) Stewart, D. Lignin as a base material for materials applications: Chemistry, application and economics. *Ind. Crop. Prod.* **2008**, *27*, 202–207.
- (7) Cateto, C. A.; Batteiro, M. F.; Rodrigues, A. E. Monitoring of lignin-based polyurethane synthesis by FTIR-ATR. *Ind. Crop. Prod.* **2008**, *27*, 168–174.
- (8) Li, Y.; Ragauskas, A. J. Kraft lignin-based rigid polyurethane foam. *J. Wood. Chem. Technol.* **2012**, *32*, 210–224.
- (9) Li, Y. Application of Cellulose Nanowhisker and Lignin in Preparation of Rigid Polyurethane Nanocomposite Foams. Ph.D. Dissertation, Georgia Institute of Technology, Atlanta, GA, 2012.
- (10) AbiSaleh, T.; et al. Introduction to Polyurethanes and Appendix 1: Calculations. In *The Huntsman Polyurethanes Book*; Randall, D., Lee, S., Eds.; Huntsman Polyurethanes: Everberg, Belgium, 2002.
- (11) Saraf, V. P.; Glasser, W. G.; Wilkes, G. L.; McGrath, J. E. Engineering plastics from lignin. VI. Structure-property relationships

of PEG-containing polyurethane networks. *J. Appl. Polym. Sci.* **1985**, *30*, 2207–2224.

- (12) Rials, T. G.; Glasser, W. G. Engineering plastics from lignin. XIII. Effect of lignin structure on polyurethane network formation. *Holzforchung* **1986**, *40*, 53–360.

- (13) Yoshida, H.; Morck, R.; Kringstad, K. P.; Hatakeyama, H. Kraft lignin in polyurethanes I. Mechanical properties of polyurethanes from a kraft lignin–polyether triol–polymeric MDI system. *J. Appl. Polym. Sci.* **1987**, *34*, 1187–1198.

- (14) Hatakeyama, T.; Matsumoto, Y.; Asano, Y.; Hatakeyama, H. Glass transition of rigid polyurethane foams derived from sodium lignosulfonate mixed with diethylene, triethylene and polyethylene glycols. *Thermochim. Acta* **2004**, *416*, 29–33.

- (15) Yoshida, H.; Morck, R.; Kringstad, K. P.; Hatakeyama, H. Kraft lignin in polyurethanes. II. Effects of the molecular weight of kraft lignin on the properties of polyurethanes from a kraft lignin–polyether triol–polymeric MDI system. *J. Appl. Polym. Sci.* **1990**, *40*, 1819–1832.

- (16) Wang, H.; Ni, Y.; Jahan, M. S.; Liu, Z.; Schafer, T. Stability of cross-linked acetic acid lignin containing polyurethane. *J. Therm. Anal. Calorim.* **2011**, *103*, 293–302.

- (17) Silva, M. C.; Takahashi, J. A.; Chaussy, D.; Belgacem, M. N.; Silva, G. G. Composites of rigid polyurethane foam and cellulose fiber residue. *J. Appl. Polym. Sci.* **2010**, *117*, 3665–3672.

- (18) Banik, I.; Sain, M. M. Structure of glycerol and cellulose fiber modified water blown soy polyol based polyurethane foams. *J. Reinf. Plast. Comp.* **2008**, *27*, 1745–1758.

- (19) Gu, R. J.; Sain, M. M.; Konar, S. K. A feasibility study of polyurethane composite foam with added hardwood pulp. *Ind. Crop. Prod.* **2013**, *42*, 273–279.

- (20) Granata, A.; Argyropoulos, D. S. 2-Chloro-4,4,5,5-tetramethyl-1,3,2-dioxaphospholite, a reagent for the accurate determination of the uncondensed and condensed phenolic moieties in lignins. *J. Agric. Food Chem.* **1995**, *43*, 1538–1544.

- (21) Pan, X. J.; Saddler, J. N. Effect of replacing polyol by organosolv and kraft lignin on the property and structure of rigid polyurethane foam. *Biotechnol. Biofuels* **2013**, *6*, 12.

- (22) Cao, X. D.; Dong, H.; Li, C. M. New nanocomposite materials reinforced with flax cellulose nanocrystals in waterborne polyurethane. *Biomacromolecules* **2007**, *8*, 899–904.

- (23) Luo, X. G.; Mohanty, A.; Misra, M. Lignin as a reactive reinforcing filler for water-blown rigid biofoam composites from soy oil-based polyurethane. *Ind. Crop. Prod.* **2013**, *47*, 13–19.

- (24) Pei, A. H.; Malho, J. M.; Ruokolainen, J.; Zhou, Q.; Berglund, L. A. Strong nanocomposite reinforcement effects in polyurethane elastomer with low volume fraction of cellulose nanocrystals. *Macromolecules* **2011**, *44*, 4422–4427.

- (25) Xue, B. L.; Wen, J. L.; Xu, F.; Sun, R. C. Polyols production by chemical modification of autocatalyzed ethanol–water lignin from *Betula alnoides*. *J. Appl. Polym. Sci.* **2013**, *129*, 434–442.

- (26) Castelvetro, V.; Geppi, M.; Giaiacopi, S.; Mollica, G. Cotton fibers encapsulated with homo- and block copolymers: Synthesis by the atom transfer radical polymerization grafting from technique and solid-state NMR dynamic investigations. *Biomacromolecules* **2007**, *8*, 498–508.

- (27) Wallace, G.; Russell, W. R.; Lomax, J. A.; Jarvis, M. C.; Lapierre, C.; Chesson, A. Extraction of phenolic–carbohydrate complexes from graminaceous cell walls. *Carbohydr. Res.* **1995**, *272*, 41–53.

- (28) Dolomanova, V.; Rauhe, J. C. Mechanical properties and morphology of nanoreinforced rigid PU foam. *J. Cell. Plast.* **2011**, *47*, 81–93.

- (29) Cui, G. J.; Fan, H. L.; Xia, W. B.; Ai, F. J.; Huang, J. Simultaneous enhancement in strength and elongation of waterborne polyurethane and role of star-like network with lignin core. *J. Appl. Polym. Sci.* **2008**, *109*, 56–63.

- (30) Lin, B.; Yang, L.; Dai, H.; Hou, Q.; Zhang, L. Thermal analysis of soybean oil based polyols. *J. Therm. Anal. Calorim.* **2009**, *95*, 977–983.